

Two-neutron transfer in the ${}^6\text{He} + {}^{120}\text{Sn}$ reaction

S. Appannababu,^{1,*} R. Lichtenthaler,¹ M. A. G. Alvarez,² M. Rodrıguez-Gallardo,² A. Lepine-Szily,¹ K. C. C. Pires,¹ O. C. B. Santos,¹ U. U. Silva,¹ P. N. de Faria,³ V. Guimares,¹ E. O. N. Zevallas,¹ V. Scarduelli,¹ M. Assuncao,⁴ J. M. B. Shorto,⁵ A. Barioni,⁶ J. Alcantara-Nunez,¹ and V. Morcelle⁷

¹*Instituto de Fısica, Universidade de Sao Paulo, 05508-090, Sao Paulo, Brazil*

²*Departamento de FAMN, Universidad de Sevilla, Apartamento 1065, E-41080 Sevilla, Spain*


³*Departamento de Fısica, Universidade Federal Fluminense do Rio de Janeiro, 24210-310 Rio de Janeiro, Brazil*

⁴*Departamento de Fısica, Universidade Federal de Sao Paulo, UNIFESP, CEP 09913-030 Diadema, Brazil*

⁵*Instituto de Pesquisas Energeticas e Nucleares, IPEN, 05508-000 Sao Paulo, Brazil*

⁶*Departamento de Ciencias do Mar, Universidade Federal de Sao Paulo, UNIFESP, Sao Paulo, Brazil*

⁷*Departamento de Fısica, Universidade Federal Rural do Rio de Janeiro, 23851-970 Rio de Janeiro, Brazil*

 (Received 13 July 2018; revised manuscript received 6 October 2018; published 4 January 2019)

A large yield of α particles produced in the ${}^{120}\text{Sn}({}^6\text{He}, \alpha)$ reaction was measured at 20.3-, 22.2-, 22.4-, and 24.5-MeV bombarding energies. The α particles are distributed over a broad energy range in the vicinity and below the elastic scattering ${}^6\text{He}$ peak. Energy integrated α -particle cross sections have been obtained at $\theta_{\text{lab}} = 36^\circ$, 40° , and 60° . The α energy distributions have been analyzed at a fixed laboratory angle ($\approx 60^\circ$) in terms of the reaction Q value, considering the $2n$ -transfer reaction kinematics ${}^{120}\text{Sn}({}^6\text{He}, \alpha){}^{122}\text{Sn}$. A kinematical analysis of the Q -value distribution shows that the recoil system ${}^{120}\text{Sn} + 2n$ is formed in highly excited states in the continuum, at increasing excitation energies as the bombarding energy increases. It is shown that by using Brink's formula, the excitation energy depends on the transferred angular momentum following a linear relation with the square of the angular momentum, indicating that some kind of dinuclear rotating system is formed after the reaction.

DOI: [10.1103/PhysRevC.99.014601](https://doi.org/10.1103/PhysRevC.99.014601)

I. INTRODUCTION

With the availability of radioactive ion beams, the study of nuclei far from the line of stability has been considerably improved. Over the last few years, elastic scattering and transfer reactions induced by low-energy neutron-rich and proton-rich projectiles on several targets have been investigated [1–6]. There were several reports showing that total reaction cross sections in reactions with radioactive ion beams are larger when compared with reactions with stable beams [2,3,5]. An important step in the study of nuclear reactions with radioactive ion beams is to identify the reaction channels responsible for the increase in the total reaction cross sections, such as breakup and transfer. Light nuclei away from the line of stability usually present a pronounced clusterlike structure formed by a core surrounded by one or more weakly bound nucleons. Several examples, such as ${}^6\text{He}(\alpha + 2n)$, ${}^{11}\text{Li}({}^9\text{Li} + 2n)$, ${}^{11}\text{Be}({}^{10}\text{Be} + n)$, ${}^{14}\text{Be}({}^{12}\text{Be} + 2n)$, and others, are found mainly in the neutron rich side of the nuclear chart. Owing to their small breakup energies and the low angular momentum of the valence neutrons, their wave functions extend to large distances from the core, forming a kind of low density neutron halo [7–10]. As a result, reactions such as projectile breakup and neutron transfers may be strongly favored in the

interaction of these projectiles with various targets, which enhances the total reaction cross sections. There have been several reports showing high total reaction cross sections in reactions involving exotic projectiles [2,3,7,11–15].

The study of nuclear reactions with ${}^6\text{He}$ has been interesting due to the observation of a large yield of α particles produced in the interaction with heavy targets [16–22]. The Borromean halo nucleus ${}^6\text{He}$ has a two-neutron separation energy of 0.975 MeV and it is expected to easily break up into an α particle and two neutrons when interacting with a target. In addition to this, the halo nature of ${}^6\text{He}$ (neutron halo) could induce neutron transfer reactions between projectile and target. The indirect effect of the projectile breakup on the elastic scattering angular distributions has been described with great success by four body continuum discretized coupled channels (4b-CDCC) calculations [3,11,23–26]. The reaction mechanism responsible for the α -particle production, on the other hand, is not yet well understood and it has been the subject of several investigations. The experimental α -production cross sections in reactions ${}^6\text{He} + {}^{209}\text{Bi}$, ${}^{238}\text{U}$ [16,17,19] are very large, well above the theoretical predictions considering the usual breakup/transfer mechanism, and are very much closer to the fusion cross sections of stable systems.

In a previous work, a large number of α particles produced in the ${}^6\text{He} + {}^{120}\text{Sn}$ reaction at energies slightly above the Coulomb barrier was observed [27,28]. In this work the experimental α -particle energy distributions were analyzed by two different models: the two-neutron transfer to the ${}^{122}\text{Sn}$

*Present address: Department of Nuclear Physics, Andhra University, Visakhapatnam 530 003, India.

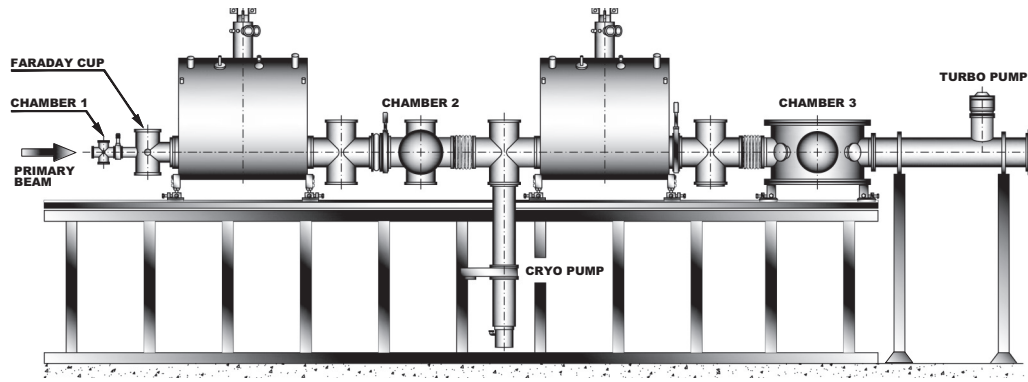


FIG. 1. Scheme of RIBRAS.

continuum (TC-DWBA) calculations and the three-body continuum discretized coupled channels (3b-CDCC) for the projectile breakup [29,30]. The magnitude of the experimental α -particle cross sections were reasonably well reproduced by the transfer to continuum (TC-DWBA) calculations, whereas the 3b-CDCC breakup calculations predict α cross sections well below the experimental values. In addition to this, the α -particle energy distributions were not well reproduced by 3b-CDCC, which gave distributions centered at energies smaller than the experimentally observed values. On the other hand, the energy distributions calculated by TC-DWBA were in better agreement with the data. However, in Ref. [27] a slight tendency was observed of the centroid of the energy distributions to shift to higher excitation energies, as the bombarding energies increased, in comparison to the TC-DWBA calculations. This motivated us to extend the measurements to higher incident energies. In this context, we performed a couple of experiments to extend the data for elastic scattering, as well as the α -production cross section for the ${}^6\text{He} + {}^{120}\text{Sn}$ reaction. In this paper, we present new data for the ${}^{120}\text{Sn}({}^6\text{He}, \alpha)X$ reaction at three different energies, $E_{\text{lab}} = 20.3, 22.4,$ and 24.5 MeV, along with the elastic scattering angular distribution studies at $E_{\text{lab}} = 22.2$ MeV. The structure of the paper is organized as follows. In Sec. II, we describe the experimental setup and the data analysis of the elastic scattering angular distributions along with the α -particle energy distributions. In Sec. III we describe the analysis of the energy distributions of the α particles supposing the kinematics of the $2n$ transfer reaction. In Sec. IV, we summarize the results and present the conclusions.

II. EXPERIMENT AND RESULTS

The experiments were performed in two phases by using the RIBRAS (Radioactive Ion Beams in Brasil) facility at São Paulo University [4–6]. A scheme of the RIBRAS setup is presented in Fig. 1. In the first phase, we measured the elastic scattering and α -particle production for the ${}^6\text{He} + {}^{120}\text{Sn}$ reaction at 22.2 MeV, by using the two solenoids of the RIBRAS facility. In the second phase we used only one solenoid to measure the α -particle production at three different energies 20.3, 22.4, and 24.5 MeV.

A primary beam of ${}^7\text{Li}^{3+}$ was used to produce in flight the secondary ${}^6\text{He}$ beam with the ${}^9\text{Be}({}^7\text{Li}, {}^6\text{He}){}^{10}\text{B}$ transfer reaction.

The ${}^7\text{Li}$ primary beam had an intensity around 300 nAe and the secondary beam had an intensity of about 10^5 pps. The ${}^7\text{Li}$ primary beam was suppressed in a Faraday cup located just after the primary target. The Faraday cup is connected to a current integrator which provides a measurement of the total number of incident primary beam particles in a run.

The ${}^6\text{He}$ particles were selected by the first solenoid and focused in the scattering chamber 2. The secondary beam at this position is contaminated with $p, d, t, \alpha,$ and ${}^7\text{Li}^{2+}$ particles coming from the degraded primary beam. A 2-mg/cm² gold foil was placed in scattering chamber 2 to provide differential energy loss and subsequent purification of the secondary beam by using the second solenoid. The gold foil also provided the charge state change from ${}^7\text{Li}^{2+}$ and a blocker (“lollipop”) was used after the second solenoid to suppress the remaining ${}^7\text{Li}^{3+}$ particles. In this way, a secondary ${}^6\text{He}$ beam with purity better than 92% was achieved in the secondary scattering chamber 3. The ${}^6\text{He}$ beam was focused on the 3.8-mg/cm²-thick ${}^{120}\text{Sn}$ secondary target using the twin solenoids [4]. The production rate of ${}^6\text{He}$ was maximized in the beginning of the experiment by varying the currents of the solenoids and monitoring the elastic scattering cross section on a ${}^{197}\text{Au}$ target after the first solenoid as well as after the second solenoid. A 4.0-mg/cm²-thick Gold target was used in secondary chamber 3 for normalization, as ${}^6\text{He} + {}^{197}\text{Au}$ scattering is pure Rutherford at the energies and angles measured in the present experiment. The elastic scattering and α -production measurements at 22.2 MeV were carried out by using four $\Delta E(25\text{--}50 \mu\text{m})\text{-}E(1000 \mu\text{m})$ silicon detector telescopes. These telescopes were mounted on a rotating plate inside secondary chamber 3, to perform angular distribution measurements. The detectors were placed at distances of 7.0–12.3 cm from the target position with a collimator opening of 5–8 msr. Figure 2 shows a bidimensional $\Delta E\text{-}E$ spectrum measured with ${}^{120}\text{Sn}$ target using the two solenoids. Measurements at 18°, 22°, 36°, 40°, 58°, 64°, 108°, and 136° have been performed at 22.2 MeV. In the backward angles 108° and 136° there were no statistics indicating that the cross sections were too small. The angular acceptance of the detectors was around $\pm 3^\circ$.

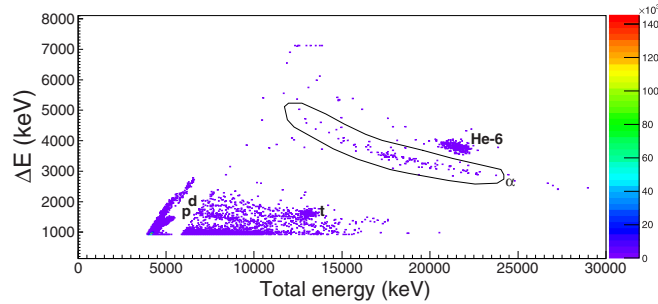


FIG. 2. ΔE - E_{total} spectrum for the reaction ${}^6\text{He} + {}^{120}\text{Sn}$ at 22.2 MeV and 36° using the two solenoids of RIBRAS.

We can clearly see that the elastically scattered ${}^6\text{He}$ peak is well separated from the α particles produced in the reaction. One can also observe in Fig. 2 the ${}^6\text{He}$, α , t , d , p peaks well separated and no contamination from the primary beam. The energy calibration was performed using an ${}^{241}\text{Am}$ source and taking the elastic scattering ${}^6\text{He}$ peak as a reference.

The elastic scattering cross section was determined from the expression

$$\sigma_{\text{cm}}^{\text{Sn}}(\theta) = \frac{N_{\text{Sn}}^c}{N_{\text{Au}}^c} \frac{N_{\text{Au}}^b}{N_{\text{Sn}}^b} \frac{N_{\text{Au}}^t}{N_{\text{Sn}}^t} \frac{J^{\text{Sn}}}{J_{\text{Au}}} \sigma_{\text{cm}}^{\text{Au}}(\theta), \quad (1)$$

where N^c is the number of counts under the peak of interest, N^b is the total number of ${}^6\text{He}$ beam particles during the run, J is the Jacobian which transforms from laboratory to the center-of-mass system, and N^t is the areal density of the target in number of atoms/cm². We consider the ratio $\frac{N_{\text{Au}}^b}{N_{\text{Sn}}^b}$ equal to the ratio of the Faraday cup integrated currents in each run. In order to monitor the production rate of the ${}^6\text{He}$ secondary beam, we perform an ${}^{197}\text{Au}$ run before and after taking a run with the Sn target. The advantage of the above expression is that it is independent of the solid angle of the detectors. The α particles present a broad energy distribution around the energy of the elastically scattered ${}^6\text{He}$ peak, confirming the previous measurements [27].

In the second phase of the experiment, we used only one solenoid to separate and focus the ${}^6\text{He}$ beam at different energies, as mentioned before. The reason for using only one solenoid at that time was that the second solenoid was momentarily not available due to constraints in the liquid helium supply. However, the previous experiment with two solenoids gave us confidence that the possible contaminations in chamber 2 were not affecting our results regarding the α -particle production.

Two silicon ΔE (25–50 μm)- E (1000 μm) telescopes were used to detect the elastically scattered ${}^6\text{He}$ and α particles. These detectors were fixed at an angle of $\pm 60^\circ$ with respect to the beam direction and at a distance of 5.0 cm from the target. One more telescope was placed at 15° with respect to the beam direction, at a distance of 8.0 cm to normalize the beam current. A typical bidimensional ΔE - E spectrum obtained at 24.5 MeV by using the single solenoid of RIBRAS is shown in Fig. 3.

In Fig. 4 we show the α -particle energy distribution for 22.2 MeV. The energy of the α particles were obtained by

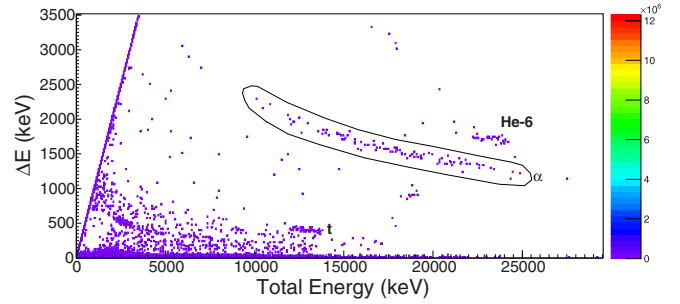


FIG. 3. ΔE - E_{total} spectrum at 60° for the ${}^6\text{He} + {}^{120}\text{Sn}$ reaction at 24.5 MeV using one solenoid of RIBRAS.

adding up the energy deposited in the ΔE , E pairs assuming that the α particles were produced in the middle of the target. Since no significant differences were observed between the α spectra at neighborhood angles, to improve the statistics, we summed the α spectra measured at 36° and 40° at 22.2 MeV.

We have analyzed the α -production data at 20.3, 22.4, and 24.5 MeV in a similar way as mentioned in the previous section, using a silicon ΔE - E telescope at forward angle (15°) to normalize the data. The α -particle energy distributions obtained at 60° in this experiment are shown in the Fig. 5 (left) along with data from previous measurements [27].

We have excluded the α data at 22.2 MeV from this figure [in Fig. 5 (left)] since the measurement at 22.2 MeV was performed at forward angles and the energy distribution depends on the angle. However the 22.2-MeV data was included in the further Q -value analysis. All the α -particle energy distributions are in the laboratory system.

Further, we plotted the α -particle energy distributions as a function of the Q value for the ${}^{120}\text{Sn}({}^6\text{He}, \alpha){}^{122}\text{Sn}^*$ reaction. The $E_\alpha \rightarrow Q_\alpha$ transformation was performed considering the two-body kinematics of the $2n$ -transfer reaction and adjusting the total reaction Q value to reproduce the measured E_α energies. In addition, the Jacobian factor dE_α/dQ has to be

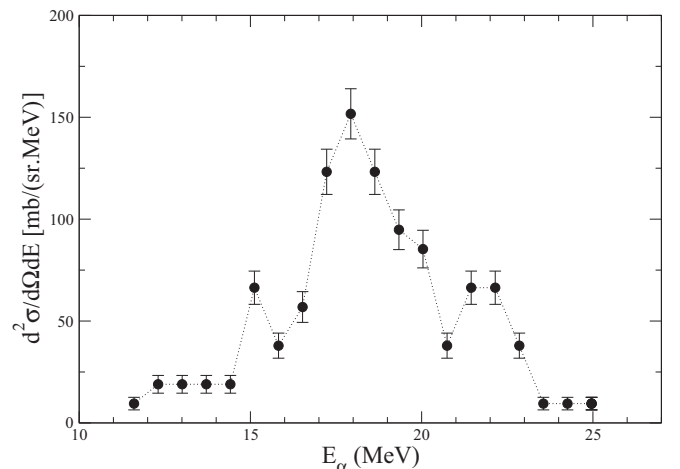


FIG. 4. Energy distribution of the α particles produced in the ${}^6\text{He} + {}^{120}\text{Sn}$ reaction at 22.2 MeV.

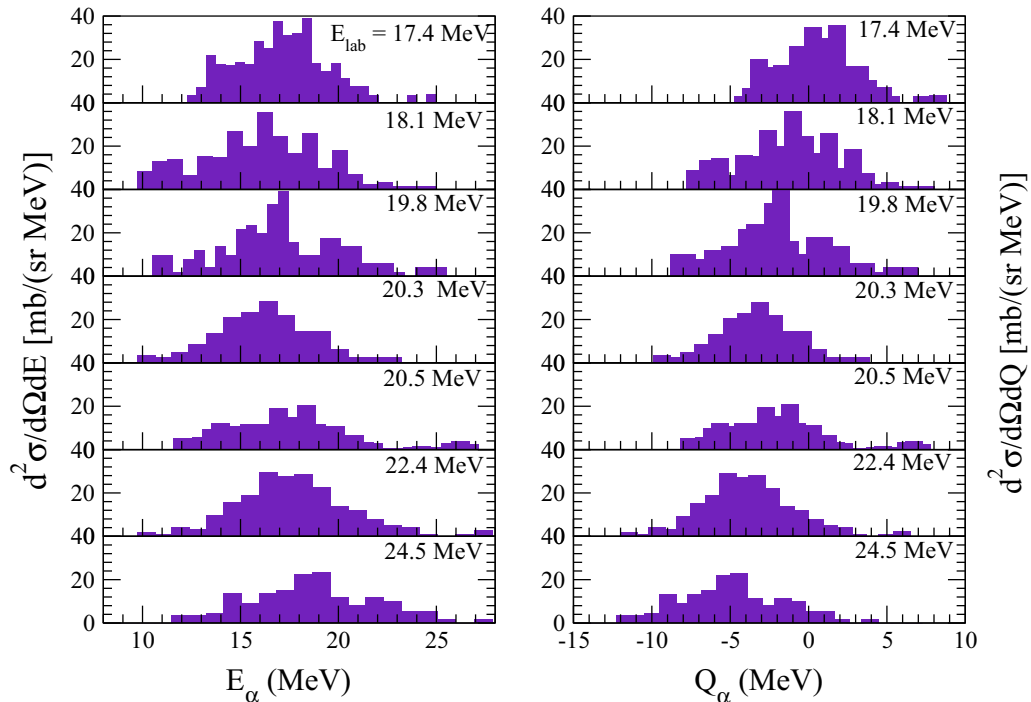


FIG. 5. Energy distribution (left) and Q -reaction distribution (right) of the α particles emitted from the $^{120}\text{Sn}(^6\text{He}, \alpha)X$ reaction, all performed at 60° . For the Q distribution the $X = ^{122}\text{Sn}$ is considered in the two-body kinematics calculation.

multiplied by the energy bin width to transform it into a Q bin. The results are presented in Fig. 5 (right).

As a result, an interesting effect can be observed in the behavior of the centroid of the Q distributions with the bombarding energies. The centroid of the Q -value distribution decreases from slightly positive values ($Q_{\text{reac}} \approx 0.3$ MeV) up to negative values around $Q_{\text{reac}} \approx -5.5$ MeV, as the incident energy increases from 17.4 to 24.5 MeV. Since $Q_{\text{reac}} = Q_{\text{gs}} - E_{\text{exc}}$ and Q_{gs} is positive ($Q_{\text{gs}} = +14.01$ MeV) the residual nucleus ^{122}Sn is formed in a highly excited state around $E_{\text{exc}} \approx 14$ MeV and above. At these high excitation energies, the $2n$ -transfer reaction populates states in the continuum of ^{122}Sn , well above the one-neutron emission threshold at $E_{\text{exc}} = 8.81$ MeV. In Table I we present the experimental energy integrated α -particle cross sections for the different bombarding energies. It is to be noted that the α -production

cross sections are of the order of two hundred mb at 60° and larger than that at more forward angles. These are large numbers compared to the CDCC breakup differential cross sections predictions which are about 10 mb around the same angles.

Some counts can be seen in the high energy part of the α distributions, in particular at 20.5 MeV. These counts are probably coming from a secondary beam of α particles produced in reactions in the primary target which have same magnetic rigidity as the ^6He secondary beam. At some energies this peak can be more or less conspicuous depending on the focusing conditions and are not to be included in the further analysis.

In Fig. 6 we present the angular distribution measured at 22.2 MeV together with four-body CDCC calculations performed in the same conditions as described in detail in Ref. [27]. Despite that only few angles were measured one observes the characteristic Fresnel rainbow diffractive pattern which is very well reproduced by the four-body CDCC calculation. It is important to mention that there are no free parameters in the present 4b-CDCC calculation and no adjustment was performed. The effect of the coupling to the continuum is shown by comparison with the dashed curve where no-coupling is considered. Although this is not a fit we calculate the total $\chi_{\text{CDCC}}^2 = 2.5$ and $\chi_{\text{no-coupling}}^2 = 6.4$ respectively for the CDCC and the no-coupling calculation. The angular distribution at 22.2 MeV shows that the α -particle measurements were performed at an angle (60°) a little bit above the grazing angle ($\theta_{\text{graz}} \approx 53^\circ$). A total reaction cross section of 2091 mb comes out from the present 4b-CDCC calculation at 22.2 MeV, in agreement with the results from Ref. [27] which range from 1491 mb at 17.4 MeV up to

TABLE I. Experimental differential α -production cross sections (energy integrated) for the $^{120}\text{Sn}(^6\text{He}, \alpha)$ reaction.

E_{lab} (MeV)	θ_{lab}	σ_α (mb)	Ref.
17.4	60	180 (43)	[27]
18.1	60	188 (33)	[27]
19.8	60	204 (44)	[27]
20.3	60	167 (19)	this work
20.5	60	160 (30)	[27]
22.2	40	380 (20)	this work
	36	500 (20)	this work
22.4	60	208 (15)	this work
24.5	60	158 (18)	this work

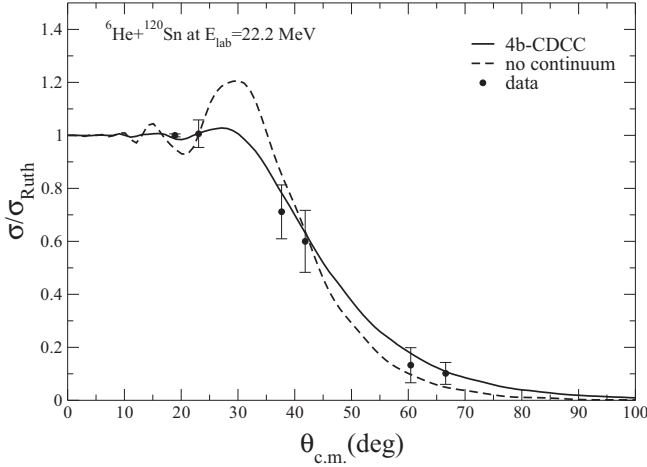


FIG. 6. ${}^6\text{He} + {}^{120}\text{Sn}$ elastic angular distributions at 22.2 MeV along with 4b-CDCC calculations.

1916 mb at 20.5 MeV. Total reaction cross sections are expected to increase with energy above the Coulomb barrier (≈ 13.3 MeV in the laboratory system).

III. ANALYSIS OF THE Q -VALUE DISTRIBUTIONS

It is well known that transfer reactions are quite selective in terms of the transferred linear and angular momentum. D. M. Brink gave the first description for this selectivity [31], in terms of two matching conditions that must be satisfied to maximize the cross section. These conditions are

$$\Delta k = k_f - k_i \approx 0 \quad (2)$$

and

$$\Delta L + \hbar \Delta \lambda = 0, \quad (3)$$

where $k_{i,f}$ are the linear momentum of the transferred particle before and after the transfer. $L = \mu v R$ is the incident orbital angular momentum and λ is the intrinsic angular momentum of the transferred particle. The first condition states that the velocity of the transferred particle must be equal before and after the collision. The second condition imposes total angular momentum conservation during the transfer process.

Considering the process $A + x \rightarrow y + B$ with $x = t + y$, t being the transferred particle, the above matching conditions can be condensed into a single equation [31]:

$$\hbar(\lambda_2 - \lambda_1) + \frac{1}{2} m_t v (R_y - R_A) + \frac{R}{v} Q = 0, \quad (4)$$

where $\Delta \lambda = (\lambda_2 - \lambda_1)$ is the transferred angular momentum, λ_1 and λ_2 are the angular momenta of the transferred particle in the initial and final nucleus, respectively, m_t is the mass of the transferred particle, v is its velocity in the position where transfer takes place, R_y and R_A are the radii of the cores y and A , and $R = R_y + R_A$ with $R_i = 1.2 A_i^{1/3}$. The local velocity is calculated by $v = \sqrt{(2(E_{\text{lab}} - V_b)/m_p)}$, where V_b is the Coulomb energy at the position where transfer takes place. We take V_b as the Coulomb barrier as given by [32,33]. For the ${}^6\text{He} + {}^{120}\text{Sn}$ system $V_b^{\text{lab}} = 13.35$ MeV. In the case of

TABLE II. Laboratory energies (MeV), Q centroids (MeV), transferred angular momentum ($\Delta \lambda$) as calculated from formula (4), excitation energies (see text), and squared final angular momentum.

E_{lab} (MeV)	Q_{av} (MeV)	$\Delta \lambda$	E_{exc} (MeV)	$\lambda_2(\lambda_2 + 1)$
17.4	0.2(3)	0.52	13.8(3)	3.83
18.1	-1.2(3)	1.94	15.2(3)	11.58
19.8	-1.8(3)	2.42	15.8(3)	15.11
20.3	-2.8(5)	3.17	16.8(5)	21.55
20.5	-2.7(5)	3.06	16.7(5)	20.54
22.2	-3.6(4)	3.60	17.6(4)	25.76
22.4	-3.5(5)	3.52	17.5(5)	24.95
24.5	-5.5(5)	4.65	19.5(5)	37.57

neutron transfers, the reaction Q value corresponds to the Q optimum, when the above condition is satisfied, and should correspond to the centroids of the Q distributions shown in Fig. 5. We obtained the centroids of the Q distributions by averaging the Q distribution at each bombarding energy: $Q_{\text{av}} = \sum(Q \times d\sigma/dQ) / \sum d\sigma/dQ$. The errors come out from a usual standard deviation calculation. The widths of the Q distributions have been also calculated and vary between 2.5 and 3 MeV but no systematic variation was seen.

In Table II we quote the laboratory energies along with the resulting Q_{av} , the corresponding transferred angular momenta $\Delta \lambda$, as deduced from Eq. (4), and the final excitation energies (see text).

Given the Q centroids we also calculate the corresponding excitation energies that are populated in the recoil nuclei: $E_{\text{exc}} = Q_{\text{gs}} - Q_{\text{av}}$ with $Q_{\text{gs}} = 14.01$ MeV being the ground state Q value for the $2n$ -transfer reaction. The errors in Q_{av} were estimated as 0.25 MeV, half width of the energy bins.

In Fig. 7, we plot the excitation energies versus the square of the intrinsic angular momentum of the final nucleus ${}^{122}\text{Sn}$, given by $\lambda_2 = \Delta \lambda + \lambda_1$, for two possible states of the angular momentum in the initial nucleus $\lambda_1 = 1$ (dots) and $\lambda_1 = 0$ (squares). The solid lines in Fig. 7 are the result of a linear

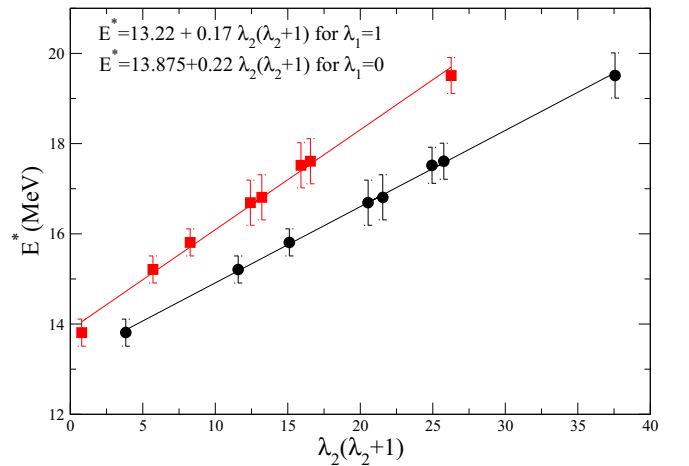


FIG. 7. Excitation energy of the final nucleus as a function of the square of the angular momentum in the final nucleus for $\lambda_1 = 1$ (dots) and $\lambda_1 = 0$ (squares). The solid line is a linear fit (see text).

data fit. The present results show, for $\lambda_1 = 1$ (dots), a linear relation between the excitation energy of the recoil nuclei and its angular momentum square $\lambda_2(\lambda_2 + 1)$. This seems to behave as a typical rotational band with $K = 13.22$ MeV and a slope $\hbar^2/(2I) = 0.17$ MeV which is very close to that expected for a rotating $2n$ - ^{120}Sn system with a moment of inertia $I = \mu R^2$ where μ is the reduced mass of the ^{120}Sn - $2n$ dinuclear system and $R = 1.2(120^{1/3} + 2^{1/3})$ fm.

The present results indicate that the experimental α -energy distributions are consistent with the formation of composite $2n$ - ^{120}Sn rotating system driven by the momentum of the transferred particle ($2n$). The dinuclear system is formed at increasing excitation energies as the bombarding energy increases, from excitation energies a little below the $2n$ threshold in the ^{122}Sn , $E_{\text{exc}} = 13.8$ MeV at $E_{\text{lab}} = 17.4$ MeV up to $E_{\text{exc}} = 19.5$ MeV at $E_{\text{lab}} = 24.5$ MeV. All these excitation energies are well above the $1n$ threshold, in the ^{122}Sn continuum, indicating that a transfer to the continuum process is taking place.

IV. SUMMARY AND CONCLUSIONS

New experimental data for α -production cross sections were presented for the reaction $^6\text{He} + ^{120}\text{Sn}$ at different energies. A large yield of α particles with a broad energy distribution has been observed in the E - ΔE spectra, in the neighborhood of the ^6He elastic scattering peak. A kinematical analysis of the α -particle energy distributions is presented in terms of the Q value for the two-neutron stripping reaction $^{120}\text{Sn}(^6\text{He}, \alpha)^{122}\text{Sn}$. The results show that the energy distributions of the α particles are centered at Q values around zero (Q optimum for neutron transfer) going to negative values $Q \approx -5.5$ MeV, as the bombarding energy increases from

17.4 to 24.5 MeV. As the $2n$ binding energy in the ^{122}Sn ground state is very much positive (+14.98 MeV), these Q values show that the recoil system $^{120}\text{Sn} + 2n$ is formed in highly excited states in the continuum. Using Brink's formula for Q optimum transfer, we tried to interpret the decrease in the reaction Q value to a corresponding increase in the transferred angular momentum. We found that the final excitation energies follow a linear relation with the square of the final angular momentum, indicating that some kind of dinuclear rotating system is formed after the collision. The moment of inertia that comes out from this relation is not far from what is expected for a $2n$ - ^{120}Sn rotating system. The α -particle production cross sections are very large indicating the presence of reaction mechanisms other than pure projectile breakup, as predicted by continuum discretized coupled channels calculations. However, it becomes clear from the present analysis that it is not possible to distinguish between different reaction mechanisms only on the basis of the α -particle energy distributions. Further measurements would be required of other degrees of freedom, such as gammas and neutrons, to decide the competition between neutron transfer or projectile breakup.

ACKNOWLEDGMENTS

This work has been partially supported by Conselho Nacional de Desenvolvimento Científico e Tecnológico–CNPq/MCTI (Brazil), Fundação de Amparo à Pesquisa do Estado de São Paulo–FAPESP (Brazil), Contracts No. 2013/22100-7 and No. 2014/19666-1. V.G. acknowledges FAPESP Grants No. 2016/17612-7 and No. 2016/02863-4. K.C.C.P. acknowledges FAPESP Process No. 2016/21434-7. M.A.G.A. would like to thank the “VI Plan Propio de Investigación”–Universidad de Sevilla (2017-2018).

-
- [1] N. Keeley, N. Alamanos, K. W. Kemper, and K. Rusek, *Prog. Part. Nucl. Phys.* **63**, 396 (2009).
- [2] E. F. Aguilera, E. Martínez-Quiroz, D. Lizcano, A. Gómez-Camacho, J. J. Kolata, L. O. Lamm, V. Guimarães, R. Lichtenthäler, O. Camargo, F. D. Becchetti, H. Jiang, P. A. DeYoung, P. J. Mears, and T. L. Belyaeva, *Phys. Rev. C* **79**, 021601(R) (2009).
- [3] V. Morcelle, R. Lichtenthäler, A. Lépine-Szily, V. Guimarães, K. C. C. Pires, J. Lubian, D. R. Mendes Junior, P. N. de Faria, J. J. Kolata, F. D. Becchetti, H. Jiang, E. F. Aguilera, D. Lizcano, E. Martínez-Quiroz, and H. Garcia, *Phys. Rev. C* **95**, 014615 (2017).
- [4] R. Lichtenthäler, M. A. G. Alvarez, A. Lépine-Szily, S. Appannababu, K. C. C. Pires, U. U. da Silva, V. Scarduelli, R. P. Condori, and N. Deshmukh, *Few-Body Syst.* **57**, 157 (2016).
- [5] A. Lépine-Szily, R. Lichtenthäler, and V. Guimarães, *Eur. Phys. J. A* **50**, 128 (2014).
- [6] R. Lichtenthäler, A. Lépine-Szily, V. Guimarães *et al.*, *Eur. Phys. J. A* **25**, 733 (2005).
- [7] I. Tanihata, H. Hamagaki, O. Hashimoto, Y. Shida, N. Yoshikawa, K. Sugimoto, O. Yamakawa, T. Kobayashi, and N. Takahashi, *Phys. Rev. Lett.* **55**, 2676 (1985).
- [8] M. Cubero, J. P. Fernández-García, M. Rodríguez-Gallardo, L. Acosta, M. Alcorta, M. A. G. Alvarez, M. J. G. Borge, L. Buchmann, C. A. Diget, H. A. Falou, B. R. Fulton, H. O. U. Fynbo, D. Galaviz, J. Gomez-Camacho, R. Kanungo, J. A. Lay, M. Madurga, I. Martel, A. M. Moro, I. Mukha *et al.*, *Phys. Rev. Lett.* **109**, 262701 (2012).
- [9] J. P. Fernández García *et al.*, *Phys. Rev. Lett.* **110**, 142701 (2013).
- [10] V. Pseudo, M. J. G. Borge, A. M. Moro, J. A. Lay, E. Nacher, J. Gomez-Camacho, O. Tengblad, L. Acosta, M. Alcorta, M. A. G. Alvarez, C. Andreou, P. C. Bender, R. Braid, M. Cubero, A. DiPietro, J. P. Fernandez-Garcia, P. Figuera, M. Fischella, B. R. Fulton, A. B. Garnsworthy *et al.*, *Phys. Rev. Lett.* **118**, 152502 (2017).
- [11] P. N. deFaria, R. Lichtenthäler, K. C. C. Pires, A. M. Moro, A. Lépine-Szily, V. Guimarães, D. R. J. Mendes, Jr., A. Arazi, M. Rodríguez-Gallardo, A. Barioni, V. Morcelle, M. C. Morais, O. Camargo, Jr., J. Alcántara Nuñez, and M. Assunção, *Phys. Rev. C* **81**, 044605 (2010).
- [12] K. C. C. Pires, R. Lichtenthäler, A. Lépine-Szily, V. Guimarães, P. N. de Faria, A. Barioni, D. R. Mendes Junior, V. Morcelle, R. Pampa Condori, M. C. Morais, J. C. Zamora, E.

- Crema, A. M. Moro, M. Rodríguez-Gallardo, M. Assunção, J. M. B. Shorto, and S. Mukherjee, *Phys. Rev. C* **83**, 064603 (2011).
- [13] K. C. C. Pires, R. Lichtenthäler, A. Lépine-Szily, and V. Morcelle, *Phys. Rev. C* **90**, 027605 (2014).
- [14] V. Morcelle *et al.*, *Phys. Lett. B* **732**, 228 (2014).
- [15] P. Mohr, D. Galaviz, Zs. Fülöp, Gy. Gyürky, G. G. Kiss, and E. Somorjai, *Phys. Rev. C* **82**, 047601 (2010).
- [16] E. F. Aguilera, J. J. Kolata, F. M. Nunes, F. D. Becchetti, P. A. DeYoung, M. Gouppell, V. Guimarães, B. Hughey, M. Y. Lee, D. Lizcano, E. Martínez-Quiroz, A. Nowlin, T. W. O'Donnell, G. F. Peaslee, D. Peterson, P. Santi, and R. White-Stevens, *Phys. Rev. Lett.* **84**, 5058 (2000).
- [17] J. P. Bychowski, P. A. DeYoung, B. B. Hilldore, J. D. Hinnefeld, A. Vida, F. D. Becchetti, J. Lupton, T. W. O'Donnell, J. J. Kolata, G. Rogachev, and M. Hencheck, *Phys. Lett. B* **596**, 26 (2004).
- [18] D. Escrig *et al.*, *Nucl. Phys. A* **792**, 2 (2007).
- [19] R. Raabe *et al.*, *Nature (London)* **431**, 823 (2004).
- [20] P. A. DeYoung, P. J. Mears, J. J. Kolata, E. F. Aguilera, F. D. Becchetti, Y. Chen, M. Cloughesy, H. Griffin, C. Guess, J. D. Hinnefeld, H. Jiang, S. R. Jones, U. Khadka, D. Lizcano, E. Martínez-Quiroz, M. Ojaniega, G. F. Peaslee, A. Pena, J. Rieth, S. VanDenDriessche, and J. A. Zimmerman, *Phys. Rev. C* **71**, 051601(R) (2005).
- [21] A. Chatterjee, A. Navin, A. Shrivastava, S. Bhattacharyya, M. Rejmund, N. Keeley, V. Nanal, J. Nyberg, R. G. Pillay, K. Ramachandran, I. Stefan, D. Bazin, D. Beaumel, Y. Blumenfeld, G. de France, D. Gupta, M. Labiche, A. Lemasson, R. Lemmon, R. Raabe, J. A. Scarpaci, C. Simenel, and C. Timis, *Phys. Rev. Lett.* **101**, 032701 (2008).
- [22] P. Mohr, P. N. deFaria, R. Lichtenthaler, K. C. C. Pires, V. Guimaraes, A. Lepine-Szily, D. R. Mendes, A. Arazi, A. Barioni, V. Morcelle, and M. C. Morais, *Phys. Rev. C* **82**, 044606 (2010).
- [23] T. Matsumoto, T. Egami, K. Ogata, Y. Iseri, M. Kamimura, and M. Yahiro, *Phys. Rev. C* **73**, 051602(R) (2006).
- [24] A. di Pietro *et al.*, *Phys. Rev. Lett.* **105**, 022701 (2010).
- [25] M. Rodríguez-Gallardo, J. M. Arias, J. Gómez-Camacho, R. C. Johnson, A. M. Moro, I. J. Thompson, and J. A. Tostevin, *Phys. Rev. C* **77**, 064609 (2008).
- [26] M. Rodríguez-Gallardo, J. M. Arias, J. Gómez-Camacho, A. M. Moro, I. J. Thompson, and J. A. Tostevin, *Phys. Rev. C* **80**, 051601(R) (2009).
- [27] P. N. de Faria, R. Lichtenthäler, K. C. C. Pires, A. M. Moro, A. Lépine-Szily, V. Guimarães, D. R. J. Mendes, Jr., A. Arazi, A. Barioni, V. Morcelle, and M. C. Morais, *Phys. Rev. C* **82**, 034602 (2010).
- [28] R. Lichtenthäler *et al.*, *EPJ Web Conf.* **69**, 00013 (2014).
- [29] I. J. Thompson, *Comput. Phys. Rep.* **7**, 167 (1988).
- [30] A. M. Moro, K. Rusek, J. M. Arias, J. Gómez-Camacho, and M. Rodríguez-Gallardo, *Phys. Rev. C* **75**, 064607 (2007).
- [31] D. M. Brink, *Phys. Lett. B* **40**, 37 (1972).
- [32] A. S. Freitas, L. Marques, X. X. Zhang, M. A. Luzio, P. Guillaumon, R. Pampa Condori, R. Lichtenthäler, *Braz. J. Phys.* **46**, 120 (2016).
- [33] K. C. C. Pires, S. Appannababu, R. Lichtenthäler, and O. C. B. Santos, *Phys. Rev. C* **98**, 014614 (2018).